



Article

Release of Pure H₂ from Na[BH₃(CH₃NH)BH₂(CH₃NH)BH₃] by Introduction of Methyl Substituents

Ting Zhang , Timothy Steenhaut , Michel Devillers and Yaroslav Filinchuk *^{*}

Institute of Condensed Matter and Nanosciences, Université Catholique de Louvain, Place Louis Pasteur 1, 1348 Louvain-la-Neuve, Belgium; ting.zhang@uclouvain.be (T.Z.)

* Correspondence: yaroslav.filinchuk@uclouvain.be

Abstract: Over the last 10 years, hydrogen-rich compounds based on five-membered boron–nitrogen chain anions have attracted attention as potential hydrogen storage candidates. In this work, we synthesized Na[BH₃(CH₃NH)BH₂(CH₃NH)BH₃] through a simple mechanochemical approach. The structure of this compound, obtained through synchrotron powder X-ray diffraction, is presented here for the first time. Its hydrogen release properties were studied by thermogravimetric analysis and mass spectrometry. It is shown here that Na[BH₃(CH₃NH)BH₂(CH₃NH)BH₃], on the contrary of its parent counterpart, Na[BH₃NH₂BH₂NH₂BH₃], is able to release up to 4.6 wt.% of pure hydrogen below 150 °C. These results demonstrate that the introduction of a methyl group on nitrogen atom may be a good strategy to efficiently suppress the release of commonly encountered undesired gaseous by-products during the thermal dehydrogenation of B-N-H compounds.

Keywords: five-membered chain anions; B-N-H compounds; mechanochemical synthesis; thermal dehydrogenation; hydrogen release

1. Introduction



Citation: Zhang, T.; Steenhaut, T.; Devillers, M.; Filinchuk, Y. Release of Pure H₂ from Na[BH₃(CH₃NH)BH₂(CH₃NH)BH₃] by Introduction of Methyl Substituents. *Inorganics* **2023**, *11*, 202. <https://doi.org/10.3390/inorganics11050202>

Academic Editor: Maurizio Peruzzini

Received: 10 April 2023

Revised: 2 May 2023

Accepted: 5 May 2023

Published: 7 May 2023



Copyright: © 2023 by the authors. Licensee MDPI, Basel, Switzerland. This article is an open access article distributed under the terms and conditions of the Creative Commons Attribution (CC BY) license (<https://creativecommons.org/licenses/by/4.0/>).

In the field of chemical hydrogen storage [1–3], boron–nitrogen–hydrogen (B-N-H) compounds have emerged as promising candidates owing to the light weight of boron and nitrogen and to their ability of bearing multiple hydrogens. Additionally, B–H and N–H bonds tend to be hydridic and protic, respectively, resulting in normally facile hydrogen release [4–10]. A typical representative of B-N-H materials is ammonia borane (NH₃BH₃, or AB), which contains three hydridic and protic hydrogens on the N and B atoms, respectively. Ammonia borane has attracted consideration attention for hydrogen storage due to its high gravimetric storage density (up to 19.6 wt.%), high stability under ambient conditions, low toxicity, and high solubility in common solvents [11–15]. However, one of the drawbacks of NH₃BH₃ for hydrogen storage is the decomposition temperature. It starts releasing the first equivalent of hydrogen at about 120 °C, and a second hydrogen elimination step occurs at approximately 145 °C; the remaining amount of hydrogen is not released until more than 500 °C. Moreover, its decomposition is exothermic and thus irreversible, and it releases multiple volatile byproducts such as NH₃, N₃B₃H₆, and B₂H₆, making the chemical hydrogenation process more challenging. In addition, the thermal decomposition of AB is furthermore paired with severe foaming and volume expansion [14,16,17]. To overcome these disadvantages, several strategies have been employed, including nanoconfinement using nanoscaffolds, catalytic effects, ionic liquid assistance, the hydrolysis reaction, and chemical modification of NH₃BH₃ through replacing one of the H atoms in the –NH₃ group of NH₃BH₃ by a metal, forming metal amidoboranes (MABs) [7,15,18–25]. Among these strategies, the formation of metal amidoboranes as a popular option show a number of advantages over neutral NH₃BH₃: (i) lower hydrogen release temperatures than that of pristine NH₃BH₃ [26]; (ii) generally the released hydrogen is not contaminated with undesirable borazine by-products [19,27,28]; (iii) the de-hydrogenation process is much less

exothermic, about 3 to 5 kJ/mol [26,29], vs. 22.5 kJ/mol for NH_3BH_3 [17,30]. Furthermore, the introduction of metals increases the diversity of hydrogen storage candidates based on B-N-H compounds. Recently, five-membered chain anions having the general formula $[\text{BH}_3\text{NH}_2\text{BH}_2\text{NH}_2\text{BH}_3]^-$, also known under the abbreviation $[\text{B}_3\text{N}_2]^-$, have emerged as a novel group of ammonia borane derivatives [31–38]. M $[\text{B}_3\text{N}_2]$ compounds have a higher hydrogen content than MABs, and the Li and Na $[\text{B}_3\text{N}_2]^-$ derivatives are stable at room temperature, on the contrary of their respective MABs [33]. However, the interest in M $[\text{B}_3\text{N}_2]$ is much more recent than for MAB, and therefore there are only few reports about their synthesis, structure, characterization, and hydrogen storage properties. In 2011, the salt of Verkade's base (2,8,9-triisobutyl-2,5,8,9-tetraaza-1-phosphabicyclo[3.3.3]undecane, $\text{C}_{18}\text{H}_{39}\text{N}_4\text{P}$, VB, chemical formula see Figure S1) with $[\text{B}_3\text{N}_2]$ was synthesized, and its structure was characterized, with the aim of studying the activating effect of VB on the rate and extent of H_2 release from NH_3BH_3 [31]. Two years later, the same authors reported the synthesis of the sodium salt and two substituted $\text{Na}[\text{BH}_3\text{N}(\text{R})\text{HBH}_2\text{N}(\text{R})\text{HBH}_3]$ salts ($\text{R} = \text{H, Me, and benzyl}$), to further study the growth of aminoborane oligomers through the de-hydrocoupling reactions of NH_3BH_3 [32]. Interestingly, since 2014, the salts of the $[\text{BH}_3\text{NH}_2\text{BH}_2\text{NH}_2\text{BH}_3]^-$ anion with different cations have been synthesized with a focus on the study of their hydrogen storage properties (see Table S1). Generally, these kinds of complexes that are studied for their hydrogen storage properties can be classified into three types, based on their cations: ionic liquids, ammonium, and alkali metal salts. A total of four $[\text{B}_3\text{N}_2]^-$ ionic liquids have been described: $[\text{Bu}_4\text{N}][\text{B}_3\text{N}_2]$, $[\text{Et}_4\text{N}][\text{B}_3\text{N}_2]$, $[\text{C}(\text{N}_3\text{H}_6)][\text{B}_3\text{N}_2]$, and $[\text{C}(\text{N}_3\text{H}_5\text{CH}_3)][\text{B}_3\text{N}_2]$ [35]. Among them, $[\text{Bu}_4\text{N}][\text{B}_3\text{N}_2]$ and $[\text{Et}_4\text{N}][\text{B}_3\text{N}_2]$ release pure hydrogen below 160 °C [35]. $[\text{NH}_4][\text{B}_3\text{N}_2]$ was reported this year, as the minor component of a 1:3 mixture with $\text{NH}_3\text{BH}_2\text{NH}_2\text{BH}_2\text{NH}_2\text{BH}_3$. Despite its impressive hydrogen content, this system releases H_2 with substantial contamination by borazine and traces of ammonia and diborane [38]. Among alkali metal (Li-Cs) salts of $[\text{B}_3\text{N}_2]^-$, only Li $[\text{B}_3\text{N}_2]$ was shown to release pure hydrogen during thermal decomposition [33,34]. However, it is the sodium salt, Na $[\text{B}_3\text{N}_2]$, that was studied the most in the literature until now, with five synthesis approaches (four wet chemical and one dry mechanochemical) reported between 2013 and 2021. In 2013, Sneddon and co-workers reported that Na $[\text{B}_3\text{N}_2]$ could be obtained from $\text{NaN}(\text{SiMe}_3)_2\text{-}3\text{ NH}_3\text{BH}_3$ in fluorobenzene at 50 °C for 24 h [32]. Grochala et al. synthesized the same compound from $\text{NaH}\text{-}3\text{NH}_3\text{BH}_3$ in THF at room temperature for 24 h and obtained Li $[\text{B}_3\text{N}_2]$ by a similar approach [33]. The same authors later used a metathesis method to obtain Na $[\text{B}_3\text{N}_2]$ from VBH $[\text{B}_3\text{N}_2]$ and M $[\text{Al}(\text{OC}(\text{CF}_3)_3)_4]$ (M = Na) in CH_2Cl_2 at room temperature for 1 h and were able to obtain the related K, Rb, and Cs salts by this method as well [34]. Although the metathesis is fast, the two precursors involved in this kind of reaction need to be synthesized first, adding a second step to the preparation of the salt. In 2021, Chen et al. reported a facile synthetic method to obtain Na $[\text{B}_3\text{N}_2]$, based on the reaction of NaNH_2BH_3 with NiBr_2 or CoCl_2 as a catalyst [36]. Results showed that the reaction with 0.05 equiv. of NiBr_2 in THF at 0 °C could produce the final Na $[\text{B}_3\text{N}_2]$ after 10 h, with a yield of 60%. The main advantages of the dry mechanochemical synthesis are that it avoids the use of solvent and usually simplifies the drying process [39,40]. However, the reported procedures for the synthesis of Li $[\text{B}_3\text{N}_2]$ and Na $[\text{B}_3\text{N}_2]$ require two stages of milling at room temperature, followed by a removal of the by-products (NH_3) upon heating [33,34]. Moreover, long time reaction times and/or complicated operating processes are usually needed for the synthesis of the alkali metal $[\text{B}_3\text{N}_2]$ compounds.

With its 12.7 wt.% hydrogen content, Na $[\text{B}_3\text{N}_2]$ has potential for hydrogen storage. However, the hydrogen released when heating this compound is contaminated by unwanted by-products, including NH_3 , B_2H_6 , and larger fragments detected by mass spectrometry [33,34]. In one of our previous studies, we found that, compared to NH_3BH_3 , the reaction of $\text{CH}_3\text{NH}_2\text{BH}_3$ with NaAlH_4 leads to a product with a completely different thermal behavior. This is likely due to the space hindrance and the electronic effect caused by the introduction of the methyl group [41]. Similar introduction of a methyl group on the N atoms of $[\text{BH}_3\text{NH}_2\text{BH}_2\text{NH}_2\text{BH}_3]^-$ in Na $[\text{B}_3\text{N}_2]$ would affect the geome-

try of the B-N-B-N-B skeleton and change the inter-anion dihydrogen bonds, potentially positively affecting the hydrogen properties of the compound. With this in mind, we synthesized $\text{Na}[\text{BH}_3(\text{CH}_3\text{NH})\text{BH}_2(\text{CH}_3\text{NH})\text{BH}_3]$ (abbreviated here as $\text{Na}[\text{B}_3(\text{MeN})_2]$) through a new convenient mechanochemical synthesis method from easily accessible NaH and $\text{CH}_3\text{NH}_2\text{BH}_3$. We also report that its structure, solved from synchrotron powder X-ray diffraction (PXRD), enables a better understanding of the structure–properties relationships. Its thermal dehydrogenation was also investigated, by thermogravimetric analysis (TGA) and mass spectrometry, revealing a release of pure hydrogen and thus confirming our hypothesis. The purity of hydrogen released from $\text{Na}[\text{BH}_3\text{NH}_2\text{BH}_2\text{NH}_2\text{BH}_3]$ was enhanced by the introduction of methyl groups on N atoms. This achievement represents the first successful suppression of the unwanted by-product release through the introduction of $-\text{CH}_3$ groups on the nitrogen atoms of $[\text{B}_3\text{N}_2]^-$. Furthermore, the structure of $\text{Na}[\text{BH}_3(\text{CH}_3\text{NH})\text{BH}_2(\text{CH}_3\text{NH})\text{BH}_3]$ was analyzed for the first time helping to understand the potential reasons behind the improved hydrogen purity. This study provides valuable insights into the relationship between the hydrogen release properties and the structure of B-N-H compounds. The introduction of methyl groups on the nitrogen atoms of $\text{Na}[\text{B}_3\text{N}_2]$ to enhance hydrogen purity could potentially be extended to the other $\text{M}[\text{B}_3\text{N}_2]$ or even other $\text{M}-\text{B}-\text{N}-\text{H}$ compound. It could even be expanded to include the use of other small alkyl groups or small electron-donating groups instead of the methyl group.

2. Results and Discussion

The reaction between NaH and NH_3BH_3 in various molar ratios was reported to produce different hydrogen rich B-N compounds, i.e., NaNH_2BH_3 (1:1), $\text{NaBH}_3\text{NH}_2\text{BH}_3$ (1:2), $\text{NaBH}_3\text{NH}_2\text{BH}_2\text{NH}_2\text{BH}_3$ (1:3), $\text{NaBH}_3\text{NH}_2\text{BH}_2\text{NH}_2\text{BH}_2\text{NH}_2\text{BH}_3$, and $\text{NaBH}_3\text{NH}_2\text{BH}(\text{NH}_2\text{BH}_3)_2$ (1:4) [42]. All of those have potential for application in hydrogen storage due to their high H content (see Table S2). Despite the potential of this system, there is only one report of the reaction between the methyl-substituted $\text{CH}_3\text{NH}_2\text{BH}_3$ and NaH , in a 1:3 molar ratio [32]. We thus investigated the reaction of NaH and $\text{CH}_3\text{NH}_2\text{BH}_3$ by mechanochemistry (Figure 1A), to avoid an incorporation of or a reaction with solvents. Upon milling $\text{NaH}-\text{CH}_3\text{NH}_2\text{BH}_3$ systems in different molar ratios, new peaks appeared on the PXRD pattern of all the tested ratios, along with some unreacted NaH for the 1:1 system (Figure 1B). The ^{11}B NMR spectra of the resulting products furthermore showed the appearance of a new quadruplet signal located between -14.45 and -16.07 ppm, which likely belongs to the BH_3 unit of $\text{Na}[\text{CH}_3\text{NHBH}_3]$. When the $\text{NaH}:\text{CH}_3\text{NH}_2\text{BH}_3$ ratio was increased to 1:2, the PXRD pattern of the obtained product shows peaks corresponding to crystalline $\text{Na}[\text{BH}_3(\text{CH}_3\text{NH})\text{BH}_2(\text{CH}_3\text{NH})\text{BH}_3]$. Although the ^{11}B NMR spectrum of the product displays a triplet signal of BH_2 (-2.24 ppm) and quadruplet signal of BH_3 (-16.39 ppm), expected for the $[\text{BH}_3(\text{CH}_3\text{NH})\text{BH}_2(\text{CH}_3\text{NH})\text{BH}_3]^-$ anion, other signals on the spectrum reveal the presence of unknown non-crystalline by-products (Figure 1C). Further increasing the ratio to 1:3 leads to the appearance of only the signals of BH_2 and BH_3 from the $[\text{BH}_3(\text{CH}_3\text{NH})\text{BH}_2(\text{CH}_3\text{NH})\text{BH}_3]^-$ anion on the ^{11}B NMR spectra. The phase purity of the compound obtained upon 27 h of ball milling the 1:3 mixture was confirmed by temperature programmed synchrotron powder X-ray diffraction (PXRD) measurements. Indeed, the complete set of peaks of the pattern disappeared at once at around 150°C (Figure S2). Based on the ^{11}B NMR spectrum and the temperature ramping synchrotron PXRD experiment, we deduce that relatively pure $\text{Na}[\text{B}_3(\text{MeN})_2]$ with five membered B-MeN-B-MeN-B chains was formed and that the reaction shown in Figure 1A was complete.

The obtained $\text{Na}[\text{B}_3(\text{MeN})_2]$ was further characterized by infrared (IR) spectroscopy (Figure 2). On the spectrum, it can be seen that the asymmetry of the N-H stretching band (3162 cm^{-1}) disappeared, compared with the $\text{CH}_3\text{NH}_2\text{BH}_3$ precursor. This is because one hydrogen on the nitrogen of $\text{CH}_3\text{NH}_2\text{BH}_3$ is released, combined with a hydride atom from NaH to form H_2 . In addition, the N-H bending of $\text{Na}[\text{B}_3(\text{MeN})_2]$ ($1457-1491\text{ cm}^{-1}$) is redshifted compared to $\text{CH}_3\text{NH}_2\text{BH}_3$ (1596 cm^{-1}). This can be attributed to the introduction

of weak electron donating methyl group on N atom, influencing the electron density of N and further having an effect on the N-H band. The broad band located in the region of 2000–2500 cm⁻¹ belongs to the B-H stretching band. There is no significant difference compared to the CH₃NH₂BH₃ precursor. However, the signal of the B-N stretching is widened and split in Na[B₃(MeN)₂] (692–716 cm⁻¹), due to the presence of two types of B-N bands in Na[B₃(MeN)₂], whereas CH₃NH₂BH₃ exhibits only one B-N band.

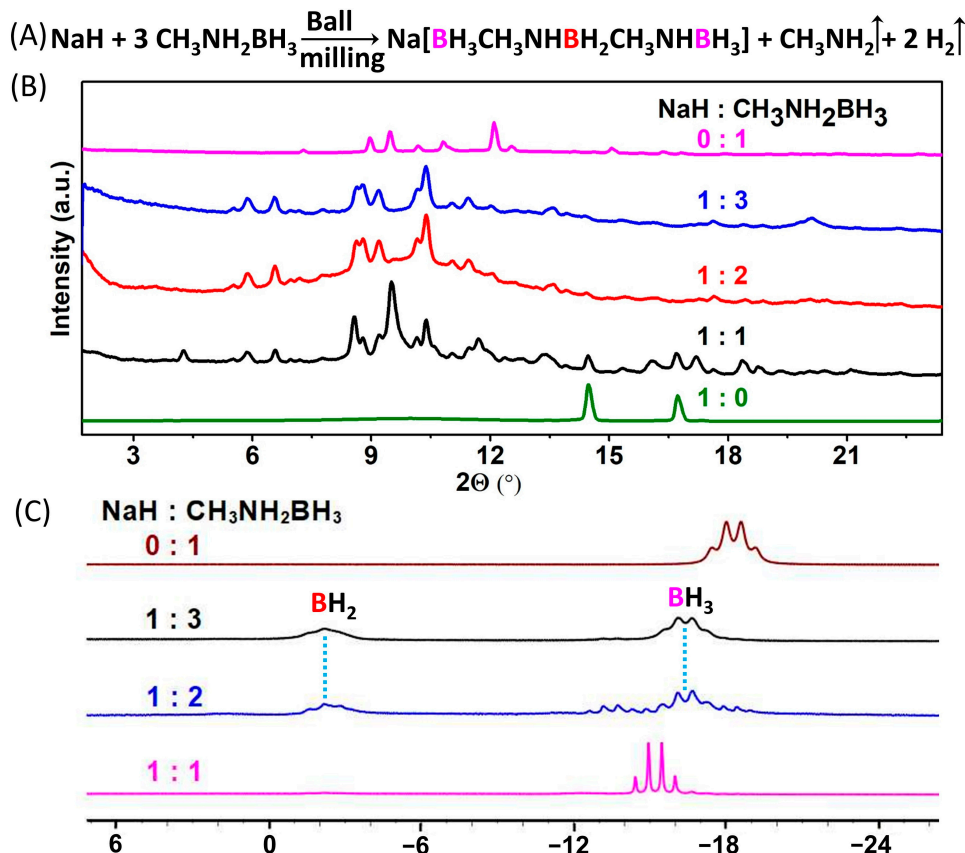


Figure 1. (A) Equation of the mechanochemical reaction; (B) PXRD patterns of NaH and CH₃NH₂BH₃ ball-milled in different molar ratios, along with patterns of NaH and CH₃NH₂BH₃ ($\lambda = 0.71073 \text{ \AA}$); (C) ^{11}B NMR spectra of ball-milled NaH and CH₃NH₂BH₃ mixtures in different molar ratios, along with the spectrum of CH₃NH₂BH₃.

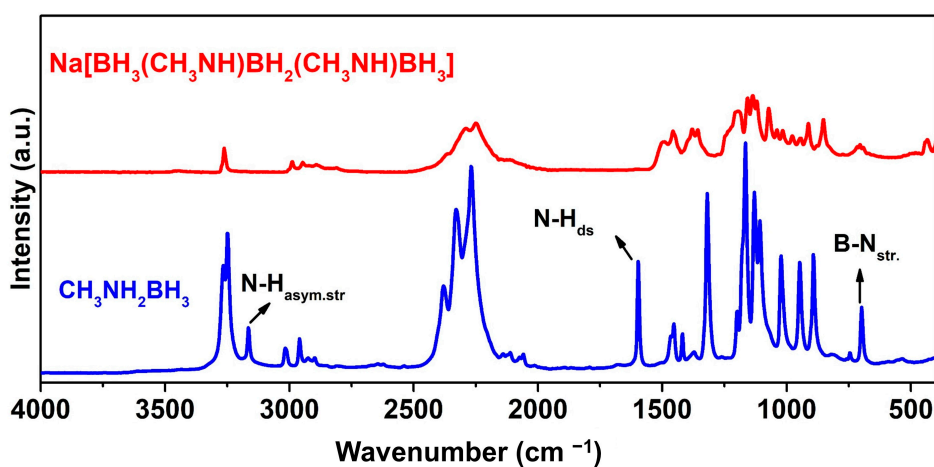


Figure 2. IR spectra of Na[B₃(MeN)₂] and CH₃NH₂BH₃.

All of the aforementioned differences between $\text{Na}[\text{B}_3(\text{MeN})_2]$ and $\text{CH}_3\text{NH}_2\text{BH}_3$ align with our previous analysis based on XRD and ^{11}B NMR, further confirming the proposed formula of the product as shown in Figure 1A.

The structure of $\text{Na}[\text{B}_3(\text{MeN})_2]$ was determined by direct space methods from synchrotron powder X-ray diffraction (PXRD) data, indexed in the monoclinic space group $P2_1/n$; the final Rietveld refinement profile is shown in Figure S3. The $[\text{BH}_3(\text{CH}_3\text{NH})\text{BH}_2(\text{CH}_3\text{NH})\text{BH}_3]^-$ anion is a five-membered B-N chain with an alternance of B and N atoms connected in a similar way as in the reported $[\text{BH}_3\text{NH}_2\text{BH}_2\text{NH}_2\text{BH}_3]^-$ [33]. Although the N atoms in $\text{Na}[\text{B}_3(\text{MeN})_2]$ have four different substituents and are therefore chiral, the crystal structure reveals that the anions are integrated in the solid as a meso compound, as both N atoms possess opposite chirality. This is in agreement with reported DFT calculations, which indicate that the meso isomer is the preferred stereoisomer for this anion [32]. Due to the introduction of the methyl substituents, the skeleton of the B-N-B-N-B chain shows a twisted geometry, which is in contrast with the linear geometry adopted by the $[\text{B}_3\text{N}_2]^-$ anion in the Li, Na, and K salts but is similar to the reported Rb and Cs $[\text{B}_3\text{N}_2]^-$ salts [34]. This type of geometry enables the formation of intramolecular dihydrogen bonds, of 2.04 and 2.12 Å (Figure 3A). With this type of geometry of the chain anion, an increase in the intramolecular interactions is expected, which should have a positive influence on the hydrogen release properties of $\text{Na}[\text{B}_3(\text{MeN})_2]$. Interanion dihydrogen bonds are also present between H atoms of the NH and terminal BH_3 groups, as well as between H atoms of the NH and the ones of the central BH_2 , as can be seen in Figure 3B and in Table S3. Unlike in the reported K $[\text{B}_3\text{N}_2]$ and Rb $[\text{B}_3\text{N}_2]$, the N-BH₂ distances are not shorter than the N-BH₃ ones (Table S4) [34,43]. Na^+ cations have a distorted triangular bipyramidal coordination geometry with five B atoms from four distinct $[\text{BH}_3(\text{CH}_3\text{NH})\text{BH}_2(\text{CH}_3\text{NH})\text{BH}_3]^-$ anions (Figure 3B,C). The coordination is performed through six hydridic H atoms of the BH_3 (green balls in Figure 3C) groups from four different chain anions. Two other hydridic H atoms from the BH_2 (red balls in Figure 3C) of one of above four chain anions complete the coordination around Na. This is different from the unsubstituted $\text{Na}[\text{BH}_3\text{NH}_2\text{BH}_2\text{NH}_2\text{BH}_3]$, where Na atoms are coordinated only to hydrogen atoms of the terminal $[\text{BH}_3]$ groups. This may be one reason of the release of large undesirable gaseous species during the thermal dehydrogenation of $\text{Na}[\text{B}_3\text{N}_2]$ [33].

The thermal stability of $\text{Na}[\text{B}_3(\text{MeN})_2]$ was investigated by thermogravimetric analysis (TGA) under inert argon atmosphere, from room temperature to 150 °C. A single step decomposition event occurs at about 80 °C, accompanied by a weight oscillation due to the so-called “jet” effect [14,44] (Figure 4A). The solid decomposition products isolated upon heating at 150 °C were identified as being crystalline NaBH_4 , along with some unknown crystalline and possibly amorphous compounds, based on PXRD and IR analyses (Figure 4B,C). Those by-products are expected to contain B, C, and N atoms, based on 4.6 wt.% the experimental weight loss as compared to 26.2 wt.% B, 19.4 wt.% C, and 22.7 wt.% N in the sample before decomposition. It is interesting to note that thermally decomposing alkali metal salts of the unsubstituted anion (Li – Cs $[\text{B}_3\text{N}_2]$) also leads to the formation of BH_4^- compounds, similarly to the title compound. The observed mass loss during the thermal decomposition of $\text{Na}[\text{B}_3(\text{MeN})_2]$, of 4.6 wt.%, is in accordance with the possible release of pure H_2 , as the compound has a theoretical hydrogen content of 8.09 wt.% (excluding H atoms from the methyl groups). This is interesting, as the parent $\text{Na}[\text{B}_3\text{N}_2]$ shows a larger mass loss (~20 wt.%) than its theoretical hydrogen content (12.7 wt.%) when heating below 200 °C, resulting in the single-step release of undesirable gaseous decomposition by-products like diborane and ammonia [34].

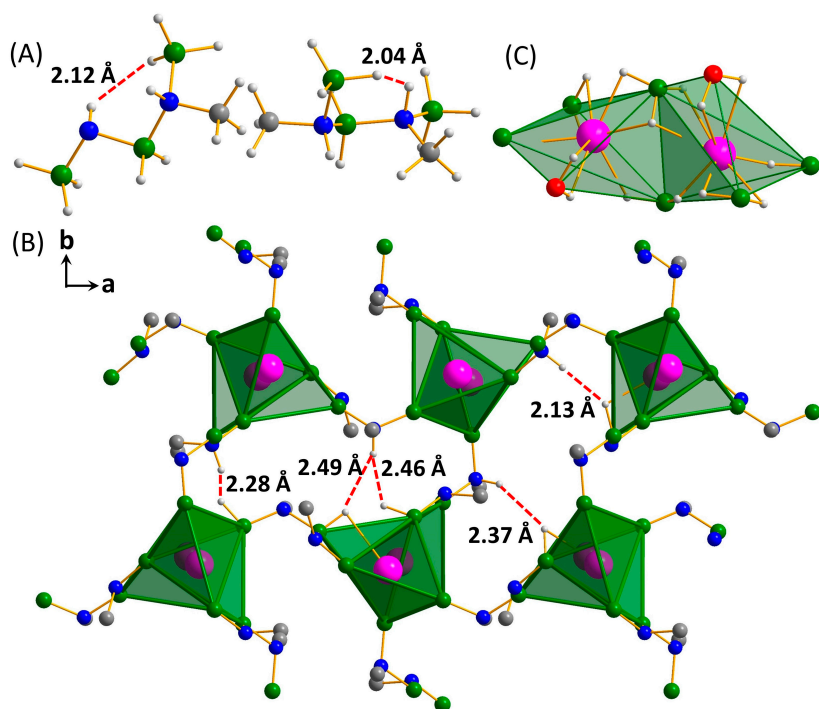


Figure 3. Ball and stick plot of the $[\text{BH}_3(\text{CH}_3\text{NH})\text{BH}_2(\text{CH}_3\text{NH})\text{BH}_3]^-$ anion with indication of the intramolecular dihydrogen bond (A), crystal packing of Na coordination polyhedra with boron atoms (hydrogen atoms are omitted for clarity) in $\text{Na}[\text{BH}_3(\text{CH}_3\text{NH})\text{BH}_2(\text{CH}_3\text{NH})\text{BH}_3]$ projected along the c axis, indicating interanion dihydrogen bonds (B), and coordination of H atoms around the Na^+ cation (central B was highlighted by red color) (C). Color code: N = blue, B = green, C = grey, H = white, and Na = pink. Dihydrogen bonds are displayed by red dotted lines.

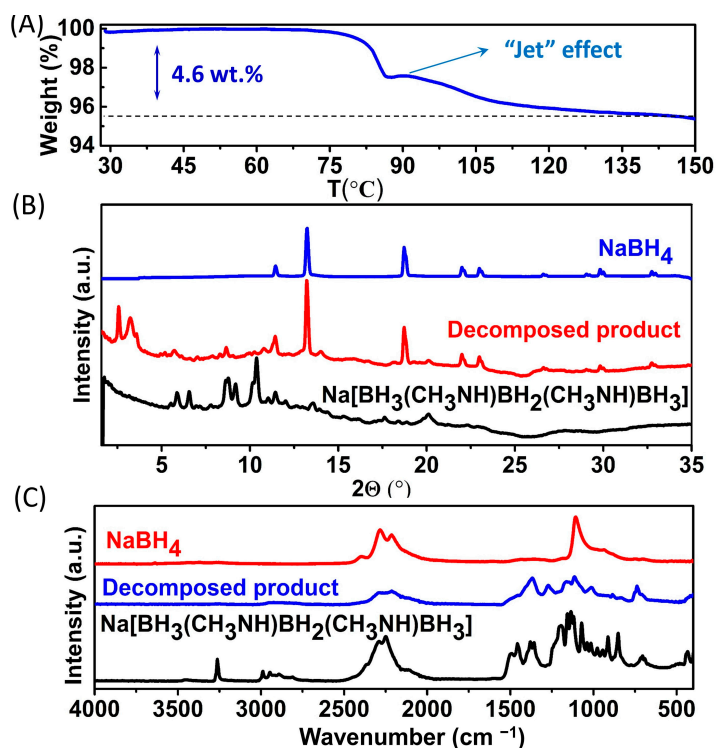


Figure 4. TG analysis of $\text{Na}[\text{B}_3(\text{MeN})_2]$ (A); PXRD patterns ($\lambda = 0.71073 \text{ \AA}$) (B) and IR spectra (C) of the product upon heating at 150°C , compared to the starting $\text{Na}[\text{B}_3(\text{MeN})_2]$ and NaBH_4 .

The purity of the gas released during the thermal de-hydrogenation of $\text{Na}[\text{B}_3(\text{MeN})_2]$ was analyzed by means of temperature-programmed mass spectrometry between 40 °C and 150 °C. Hydrogen was the only gas detected, and the experiment confirmed that NH_3 , B_2H_6 , CH_4 , and CH_3NH_2 were not released during the decomposition (Figure 5). This confirms that the methyl-substituted $\text{Na}[\text{B}_3(\text{MeN})_2]$ indeed releases about 4.6 wt.% of pure hydrogen upon heating to 150 °C. This confirmed that the introduction of a methyl group on the nitrogen atoms efficiently suppresses the release of unwanted by-products during thermal hydrogen desorption.

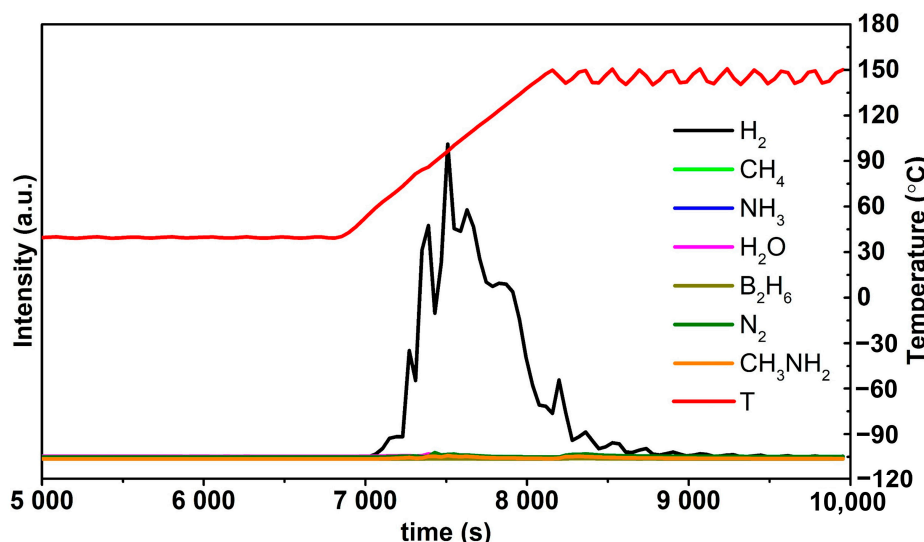


Figure 5. Mass spectrometry analysis of gases released during the thermal decomposition of $\text{Na}[\text{B}_3(\text{MeN})_2]$ under argon, between 40 °C and 150 °C.

3. Materials and Methods

All samples were obtained from commercially available NaH (95%), NaBH_4 (97%), $\text{CH}_3\text{NH}_2\cdot\text{HCl}$ (98%), and anhydrous THF ($\geq 99.9\%$) that were purchased from Sigma Aldrich Co., Ltd. (St. Louis, MI, USA). All operations were performed in gloveboxes with a high purity argon atmosphere.

3.1. Syntheses

Synthesis of $\text{CH}_3\text{NH}_2\text{BH}_3$: $\text{CH}_3\text{NH}_2\text{BH}_3$ was synthesized following a procedure adapted from the literature [45]. Initially, powdered NaBH_4 (3.79 g, 0.1 mol), $\text{CH}_3\text{NH}_2\cdot\text{HCl}$ (13.50 g, 0.1 mol), and THF (300 mL) were added to a 500 mL three-neck round-bottom flask. The resulting mixture was then vigorously stirred at ambient temperature under an argon atmosphere for 48 h. Filtration was performed to remove the solid by-product (NaCl) from the reaction mixture, and the collected filtrate was subjected to evaporation under reduced pressure using a rotary evaporator. The resulting white solid of $\text{CH}_3\text{NH}_2\text{BH}_3$ was then dried under vacuum overnight to eliminate any residual THF. The purity of the product was confirmed through characterization using ^1H , ^{11}B , and ^{13}C NMR and PXRD, as depicted in Figures S4–S7.

Synthesis of $\text{Na}[\text{BH}_3(\text{CH}_3\text{NH})\text{BH}_2(\text{CH}_3\text{NH})\text{BH}_3]$: Totals of 1 eq. of NaH (30.0 mg) and 3 eqs. of $\text{CH}_3\text{NH}_2\text{BH}_3$ (168.4 mg) were placed into an 80 mL stainless steel vial with three 10 mm diameter stainless steel balls (ball-to-powder mass ratio of 60:1). The reactants were then milled in a planetary ball mill (Fritsch Pulverisette 7 Premium line), with a rotation speed of 500 rpm for 55 milling cycles of 30 min interrupted by 5 min cooling breaks. The product was obtained as a white powder.

3.2. Instrumental

Samples were carefully filled into 0.7 mm thin-walled glass capillaries (Hilgenberg GmbH, Malsfeld, Germany) within an argon-filled glovebox. To prevent contact with air, the capillaries were sealed with grease before being taken out of the glovebox. The sealed capillaries were then cut and promptly placed into wax on a goniometer head, ensuring that no air entered the capillary. Diffraction data were immediately collected using a MAR345 image-plate detector equipped with an Incoatec Mo ($\lambda = 0.71073 \text{ \AA}$) Microfocus (1 μs 2.0) X-ray source operating at 50 kV and 1000 μA . The resulting two-dimensional images were azimuthally integrated using the Fit2D software, with LaB₆ serving as a calibrant.

Synchrotron PXRD patterns were collected with a PILATUS@SNBL diffractometer (SNBL, ESRF, Grenoble, France) equipped with a Dectris PILATUS 2M single-photon counting pixel area detector ($\lambda = 0.77509 \text{ \AA}$). Powder patterns were obtained by using raw data processed by the SNBL Toolbox software using data for LaB₆ standard. The synchrotron PXRD data for Na[BH₃(CH₃NH)BH₂(CH₃NH)BH₃] were indexed in a monoclinic unit cell, and its structure was solved by global optimization using the FOX software [46]. The anions were modeled by conformationally free z-matrices with restrained bond distances and angles. Since the N-atom of methylamidoborane is chiral, all combinations of these chiral centres were examined. The final structure showed the best fit to the data but also satisfied crystal-chemical expectations, such as the formation of dihydrogen bonds (N-H \cdots H-B) and the coordination of Na⁺ to H atoms of BH₃ and BH₂ groups. Rietveld refinements were done in Fullprof [47], refining all non-hydrogen atoms of the anions individually using restraints from DFT-refined geometry. Hydrogen atoms were refined using the rigiding model, with Na as free atoms. The symmetry was confirmed with ADDSYM routine in the PLATON software. $R_B = 7.9\%$, $R_p = 14.2$, $R_{wp} = 12.5$, $\chi^2 = 424$ (mind that the counting statistics is very high).

Fourier transform infrared spectroscopy (FTIR): Attenuated total reflectance (ATR)-IR spectra were recorded using a Bruker Alpha spectrometer. The spectrometer was equipped with a Platinum ATR sample holder, which featured a diamond crystal for single bounce measurements. The entire experimental setup was located within an argon-filled glovebox to maintain an inert atmosphere during the measurements.

Thermogravimetric analysis (TGA): TGA measurements were conducted using a Netzsch STA 449 F3 TGA/DSC. The TGA/DSC was equipped with a stainless-steel oven and located within an argon-filled glovebox to ensure an inert atmosphere during the measurements. The samples were loaded into Al₂O₃ crucibles and subjected to a heating rate of 5 K/min under an argon flow of 100 mL/min.

Mass spectrometry: Mass spectrometry measurements were conducted using a Hiden Catlab reactor coupled with a Quantitative Gas Analyser (QGA) Hiden quadrupole mass spectrometer. Prior to the experiment, the samples were loaded into a quartz tube with two layers of quartz wool, all within the protective atmosphere of an argon-filled glovebox. The ends of the quartz tube were sealed with Parafilm before being removed from the glovebox. Subsequently, the quartz tube was placed in the sample holder outside the glovebox after quickly removing the Parafilm. The argon flow (40 mL/min) was immediately initiated to prevent any contact of the sample with air. The samples were then heated to 40 °C and held isothermally for approximately 2 h to stabilize the temperature. Heating was then performed at a rate of 5 °C/min until reaching 150 °C, followed by a 1 h isotherm. Gas evolution was monitored by recording the peak with the highest intensity for each gas, specifically the m/z values of 2, 15, 17, 18, 26, 28, and 30, corresponding to H₂, CH₄, NH₃, H₂O, B₂H₆, N₂, and CH₃NH₂, respectively. The absence of H₂O and N₂ signals in the collected data confirmed the absence of leaks, ensuring that the sample remained under a protective argon atmosphere throughout the measurement.

4. Conclusions

We synthesized Na[BH₃(CH₃NH)BH₂(CH₃NH)BH₃] (Na[B₃(MeN)₂]), 130.5 g H₂/kg, 126 g H₂/L, Table S5), a methyl-substituted Na salt with five-membered B-N chain anions,

by a novel mechanochemical approach from NaH and $\text{CH}_3\text{NH}_2\text{BH}_3$. Its crystal structure was determined for the first time based on synchrotron PXRD, showing that the introduction of - CH_3 groups on the N atoms leads to the introduction of the anion in a kinked geometry into the solid, unlike its unsubstituted parent counterpart ($\text{Na}[\text{B}_3\text{N}_2]$), that possesses straight B-N chains. $\text{Na}[\text{B}_3(\text{MeN})_2]$ releases up to 4.6 wt.% of pure hydrogen below to 150 °C, contrary to its unsubstituted analogue that releases undesirable gaseous by-products during heating. This indicates that the introduction of methyl (or other) substituents on the nitrogen atoms of similar compounds is a promising approach to suppress the release of unwanted volatile by-products during thermal hydrogen release.

Supplementary Materials: The following supporting information can be downloaded at: <https://www.mdpi.com/article/10.3390/inorganics11050202/s1>, Figure S1: Chemical formula of VB; Table S1: H-contents, mass losses and by-products formed during thermal treatment of several $\text{M}[\text{B}_3\text{N}_2]$ compounds; Table S2: H-content in NaNH_2BH_3 , $\text{NaBH}_3\text{NH}_2\text{BH}_3$, $\text{NaBH}_3\text{NH}_2\text{BH}_2\text{NH}_2\text{BH}_3$, $\text{NaBH}_3\text{NH}_2\text{BH}_2\text{NH}_2\text{BH}_2\text{NH}_2\text{BH}_3$, and $\text{NaBH}_3\text{NH}_2\text{BH}(\text{NH}_2\text{BH}_3)_2$; Table S3. Inter-anion dihydrogen bond lengths and angles in $\text{Na}[\text{B}_3(\text{MeN})_2]$; Figure S2: temperature ramping synchrotron PXRD patterns of $\text{Na}[\text{B}_3(\text{MeN})_2]$; Figure S3: Rietveld refinement of the synchrotron PXRD pattern of $\text{Na}[\text{B}_3(\text{MeN})_2]$; Table S4: B-N bond lengths in $\text{CH}_3\text{NH}_2\text{BH}_3$, $\text{M}[\text{B}_3\text{N}_2]$ ($\text{M} = \text{Li} - \text{Cs}$), and $\text{Na}[\text{B}_3(\text{MeN})_2]$; Figures S4–S7: NMR and PXRD of $\text{CH}_3\text{NH}_2\text{BH}_3$; Table S5: The mole mass, density, and gravimetric and volumetric hydrogen density of $\text{Na}[\text{B}_3(\text{MeN})_2]$.

Author Contributions: Conceptualization, software, T.Z. and Y.F.; methodology, validation, formal analysis, investigation, data curation, writing—original draft preparation, and visualization, T.Z.; writing—review and editing, T.S., M.D. and Y.F., supervision, M.D. and Y.F.; project administration, funding acquisition, Y.F. All authors have read and agreed to the published version of the manuscript.

Funding: This work was supported by the FNRS (CC J.0073.20, EQP U.N038.13, EQP U.N022.19) and the Communauté Française de Belgique (ARC 18/23-093). Ting Zhang was supported through the China Scholarship Council fellowship (201809370045).

Data Availability Statement: CCDC number: 2254456 contains supplementary crystallographic data for this paper. This data can be obtained free of charge from The Cambridge Crystallographic Data Center.

Acknowledgments: We thank the ESRF for the beamtime allocation at the SNBL. We also thank François Devred for help with the mass spectrometry measurements.

Conflicts of Interest: The authors declare no conflict of interest.

References

- Chen, Z.; Ma, Z.; Zheng, J.; Li, X.; Akiba, E.; Li, H.-W. Perspectives and Challenges of Hydrogen Storage in Solid-State Hydrides. *Chin. J. Chem. Eng.* **2021**, *29*, 1–12. [[CrossRef](#)]
- Milanese, C.; Jensen, T.; Hauback, B.; Pistidda, C.; Dornheim, M.; Yang, H.; Lombardo, L.; Zuettel, A.; Filinchuk, Y.; Ngene, P.; et al. Complex Hydrides for Energy Storage. *Int. J. Hydrogen Energy* **2019**, *44*, 7860–7874. [[CrossRef](#)]
- Dematteis, E.M.; Amdisen, M.B.; Autrey, T.; Barale, J.; Bowden, M.; Buckley, C.; Cho, Y.W.; Deledda, S.; Dornheim, M.; de Jongh, P.; et al. Hydrogen Storage in Complex Hydrides: Past Activities and New Trends. *Prog. Energy* **2022**, *4*, 032009. [[CrossRef](#)]
- Huang, Z.; Autrey, T. Boron–Nitrogen–Hydrogen (BNH) Compounds: Recent Developments in Hydrogen Storage, Applications in Hydrogenation and Catalysis, and New Syntheses. *Energy Environ. Sci.* **2012**, *5*, 9257–9268. [[CrossRef](#)]
- Hamilton, C.W.; Baker, R.T.; Staubitz, A.; Manners, I. B–N Compounds for Chemical Hydrogen Storage. *Chem. Soc. Rev.* **2009**, *38*, 279–293. [[CrossRef](#)] [[PubMed](#)]
- Wang, K.; Pan, Z.; Yu, X. Metal B–N–H Hydrogen-Storage Compound: Development and Perspectives. *J. Alloys Compd.* **2019**, *794*, 303–324. [[CrossRef](#)]
- Castilla-Martinez, C.A.; Moury, R.; Demirci, U.B. Amidoboranes and Hydrazinidoboranes: State of the Art, Potential for Hydrogen Storage, and Other Prospects. *Int. J. Hydrogen Energy* **2020**, *45*, 30731–30755. [[CrossRef](#)]
- Kumar, R.; Karkamkar, A.; Bowden, M.; Autrey, T. Solid-State Hydrogen Rich Boron–Nitrogen Compounds for Energy Storage. *Chem. Soc. Rev.* **2019**, *48*, 5350–5380. [[CrossRef](#)]
- Dovgaliuk, I.; Filinchuk, Y. Aluminium Complexes of B- and N-Based Hydrides: Synthesis, Structures and Hydrogen Storage Properties. *Int. J. Hydrogen Energy* **2016**, *41*, 15489–15504. [[CrossRef](#)]

10. Paskevicius, M.; Jepsen, L.H.; Schouwink, P.; Černý, R.; Ravnsbæk, D.B.; Filinchuk, Y.; Dornheim, M.; Besenbacher, F.; Jensen, T.R. Metal Borohydrides and Derivatives—Synthesis, Structure and Properties. *Chem. Soc. Rev.* **2017**, *46*, 1565–1634. [CrossRef] [PubMed]
11. Stephens, F.H.; Pons, V.; Tom Baker, R. Ammonia–Borane: The Hydrogen Source Par Excellence? *Dalton Trans.* **2007**, *2613–2626*. [CrossRef]
12. Demirci, U.B. Ammonia Borane, a Material with Exceptional Properties for Chemical Hydrogen Storage. *Int. J. Hydrogen Energy* **2017**, *42*, 9978–10013. [CrossRef]
13. Akbayrak, S.; Özkar, S. Ammonia Borane as Hydrogen Storage Materials. *Int. J. Hydrogen Energy* **2018**, *43*, 18592–18606. [CrossRef]
14. Staubitz, A.; Robertson, A.P.M.; Manners, I. Ammonia-Borane and Related Compounds as Dihydrogen Sources. *Chem. Rev.* **2010**, *110*, 4079–4124. [CrossRef] [PubMed]
15. Wang, K.; Zhang, J.-G.; Man, T.-T.; Wu, M.; Chen, C.-C. Recent Process and Development of Metal Aminoborane. *Chem. Asian J.* **2013**, *8*, 1076–1089. [CrossRef]
16. Demirci, U.B. Mechanistic Insights into the Thermal Decomposition of Ammonia Borane, a Material Studied for Chemical Hydrogen Storage. *Inorg. Chem. Front.* **2021**, *8*, 1900–1930. [CrossRef]
17. Baitalow, F.; Baumann, J.; Wolf, G.; Jaenicke-Rößler, K.; Leitner, G. Thermal Decomposition of B–N–H Compounds Investigated by Using Combined Thermoanalytical Methods. *Thermochim. Acta* **2002**, *391*, 159–168. [CrossRef]
18. Chua, Y.S.; Chen, P.; Wu, G.; Xiong, Z. Development of Amidoboranes for Hydrogen Storage. *Chem. Commun.* **2011**, *47*, 5116–5129. [CrossRef] [PubMed]
19. Owarzany, R.; Leszczyński, J.P.; Fijalkowski, J.K.; Grochala, W. Mono- and Bimetalic Amidoboranes. *Crystals* **2016**, *6*, 88. [CrossRef]
20. Hügle, T.; Hartl, M.; Lentz, D. The Route to a Feasible Hydrogen-Storage Material: MOFs Versus Ammonia Borane. *Eur. J. Chem.* **2011**, *17*, 10184–10207. [CrossRef]
21. Li, L.; Yao, X.; Sun, C.; Du, A.; Cheng, L.; Zhu, Z.; Yu, C.; Zou, J.; Smith, S.C.; Wang, P.; et al. Lithium-Catalyzed Dehydrogenation of Ammonia Borane within Mesoporous Carbon Framework for Chemical Hydrogen Storage. *Adv. Funct. Mater.* **2009**, *19*, 265–271. [CrossRef]
22. Huang, X.; Liu, Y.; Wen, H.; Shen, R.; Mehdi, S.; Wu, X.; Liang, E.; Guo, X.; Li, B. Ensemble-boosting effect of Ru–Cu alloy on catalytic activity towards hydrogen evolution in ammonia borane hydrolysis. *Appl. Catal. B* **2021**, *287*, 119960. [CrossRef]
23. Kang, N.; Wei, X.; Shen, R.; Li, B.; Cal, E.G.; Moya, S.; Salmon, L.; Wang, C.; Coy, E.; Berlande, M.; et al. Fast Au–Ni@ZIF-8-catalyzed ammonia borane hydrolysis boosted by dramatic volcano-type synergy and plasmonic acceleration. *Appl. Catal. B* **2023**, *320*, 121957. [CrossRef]
24. Mehdi, S.; Liu, Y.; Wei, H.; Zhang, H.; Shen, R.; Guan, S.; Wu, X.; Liu, T.; Wen, H.; Peng, Z.; et al. P-induced Co-based interfacial catalysis on Ni foam for hydrogen generation from ammonia borane. *Appl. Catal. B* **2023**, *325*, 122317. [CrossRef]
25. Himmelberger, D.W.; Yoon, C.W.; Bluhm, M.E.; Carroll, P.J.; Sneddon, L.G. Base-Promoted Ammonia Borane Hydrogen-Release. *J. Am. Chem. Soc.* **2009**, *131*, 14101–14110. [CrossRef]
26. Xiong, Z.; Yong, C.K.; Wu, G.; Chen, P.; Shaw, W.; Karkamkar, A.; Autrey, T.; Jones, M.O.; Johnson, S.R.; Edwards, P.P.; et al. High-Capacity Hydrogen Storage in Lithium and Sodium Amidoboranes. *Nat. Mater.* **2007**, *7*, 138–141. [CrossRef]
27. Diyabalanage, H.V.K.; Nakagawa, T.; Shrestha, R.P.; Semelsberger, T.A.; Davis, B.L.; Scott, B.L.; Burrell, A.K.; David, W.I.F.; Ryan, K.R.; Jones, M.O.; et al. Potassium(I) Amidotrihydroborate: Structure and Hydrogen Release. *J. Am. Chem. Soc.* **2010**, *132*, 11836–11837. [CrossRef]
28. Luo, J.; Kang, X.; Wang, P. Synthesis, Formation Mechanism, and Dehydrogenation Properties of the Long-Sought $Mg(NH_2BH_3)_2$ Compound. *Energy Environ. Sci.* **2013**, *6*, 1018–1025. [CrossRef]
29. Diyabalanage, H.V.K.; Shrestha, R.P.; Semelsberger, T.A.; Scott, B.L.; Bowden, M.E.; Davis, B.L.; Burrell, A.K. Calcium Amidotrihydroborate: A Hydrogen Storage Material. *Angew. Chem. Int. Ed.* **2007**, *46*, 8995–8997. [CrossRef]
30. Wolf, G.; Baumann, J.; Baitalow, F.; Hoffmann, F.P. Calorimetric Process Monitoring of Thermal Decomposition of B–N–H Compounds. *Thermochim. Acta* **2000**, *343*, 19–25. [CrossRef]
31. Ewing, W.C.; Marchione, A.; Himmelberger, D.W.; Carroll, P.J.; Sneddon, L.G. Syntheses and Structural Characterizations of Anionic Borane-Capped Ammonia Borane Oligomers: Evidence for Ammonia Borane H_2 Release Via a Base-Promoted Anionic Dehydropolymerization Mechanism. *J. Am. Chem. Soc.* **2011**, *133*, 17093–17099. [CrossRef]
32. Ewing, W.C.; Carroll, P.J.; Sneddon, L.G. Syntheses and Characterizations of Linear Triborazanes. *Inorg. Chem.* **2013**, *52*, 10690–10697. [CrossRef] [PubMed]
33. Fijalkowski, K.J.; Jaroń, T.; Leszczyński, P.J.; Magos-Palasyuk, E.; Palasyuk, T.; Cyrański, M.K.; Grochala, W. $M(BH_3NH_2BH_2NH_2BH_3)$ —The Missing Link in the Mechanism of the Thermal Decomposition of Light Alkali Metal Amidoboranes. *Phys. Chem. Chem. Phys.* **2014**, *16*, 23340–23346. [CrossRef] [PubMed]
34. Owarzany, R.; Fijalkowski, K.J.; Jaroń, T.; Leszczyński, P.J.; Dobrzycki, Ł.; Cyrański, M.K.; Grochala, W. Complete Series of Alkali-Metal $M(BH_3NH_2BH_2NH_2BH_3)$ Hydrogen-Storage Salts Accessed via Metathesis in Organic Solvents. *Inorg. Chem.* **2016**, *55*, 37–45. [CrossRef] [PubMed]
35. Chen, X.-M.; Jiang, X.; Jing, Y.; Chen, X. Synthesis and Dehydrogenation of Organic Salts of a Five-Membered B/N Anionic Chain, a Novel Ionic Liquid. *Chem. Asian J.* **2021**, *16*, 2475–2480. [CrossRef] [PubMed]

36. Ju, M.-Y.; Guo, Y.; Chen, X.-M.; Chen, X. Facile Synthetic Method of $\text{Na}[\text{BH}_3(\text{NH}_2\text{BH}_2)_2\text{H}]$ Based on the Reactions of Sodium Amidoborane (NaNH_2BH_3) with NiBr_2 or CoCl_2 . *Inorg. Chem.* **2021**, *60*, 7101–7107. [[CrossRef](#)]
37. Nawrocka, E.K.; Prus, A.; Owarzany, R.; Koźmiński, W.; Kazimierczuk, K.; Fijałkowski, K.J. The Assignment of ^{11}B and ^1H Resonances in the Post-Reaction Mixture from the Dry Synthesis of $\text{Li}(\text{BH}_3\text{NH}_2\text{BH}_2\text{NH}_2\text{BH}_3)$. *Magn. Reson. Chem.* **2023**, *61*, 49–54. [[CrossRef](#)]
38. Owarzany, R.; Jaroń, T.; Kazimierczuk, K.; Malinowski, P.J.; Grochala, W.; Fijałkowski, K.J. In Towards Hydrogen-Rich Ionic (NH_4) $(\text{BH}_3\text{NH}_2\text{BH}_2\text{NH}_2\text{BH}_3)$ and Related Molecular $\text{NH}_3\text{BH}_2\text{NH}_2\text{BH}_2\text{NH}_2\text{BH}_3$. *Dalton Trans.* **2023**, *52*, 3586–3595. [[CrossRef](#)]
39. James, S.L.; Adams, C.J.; Bolm, C.; Braga, D.; Collier, P.; Friščić, T.; Grepioni, F.; Harris, K.D.M.; Hyett, G.; Jones, W.; et al. Mechanochemistry: Opportunities for New and Cleaner Synthesis. *Chem. Soc. Rev.* **2012**, *41*, 413–447. [[CrossRef](#)]
40. Do, J.-L.; Friščić, T. Mechanochemistry: A Force of Synthesis. *ACS Cent. Sci.* **2017**, *3*, 13–19. [[CrossRef](#)]
41. Zhang, T.; Steenhaut, T.; Li, X.; Devred, F.; Devillers, M.; Filinchuk, Y. Aluminum Methylamidoborane Complexes: Mechanochemical Synthesis, Structure, Stability, and Reactive Hydride Composites. *Sustain. Energy Fuels* **2023**, *7*, 1119–1126. [[CrossRef](#)]
42. Chen, X.-M.; Wang, J.; Liu, S.-C.; Zhang, J.; Wei, D.; Chen, X. Controllable Syntheses of B/N Anionic Aminoborane Chain Complexes by the Reaction of NH_3BH_3 with NaH and the Mechanistic Study. *Dalton Trans.* **2019**, *48*, 14984–14988. [[CrossRef](#)] [[PubMed](#)]
43. Bowden, M.E.; Brown, I.W.M.; Gainsford, G.J.; Wong, H. Structure and Thermal Decomposition of Methylamine Borane. *Inorganica Chim. Acta* **2008**, *361*, 2147–2153. [[CrossRef](#)]
44. Dovgaliuk, I.; Jepsen, L.H.; Safin, D.A.; Łodziana, Z.; Dyadkin, V.; Jensen, T.R.; Devillers, M.; Filinchuk, Y. A Composite of Complex and Chemical Hydrides Yields the First Al-Based Amidoborane with Improved Hydrogen Storage Properties. *Eur. J. Chem.* **2015**, *21*, 14562–14570. [[CrossRef](#)]
45. Dovgaliuk, I.; Møller, K.T.; Robeyns, K.; Louppe, V.; Jensen, T.R.; Filinchuk, Y. Complexation of Ammonia Boranes with Al^{3+} . *Inorg. Chem.* **2019**, *58*, 4753–4760. [[CrossRef](#)]
46. Favre-Nicolin, V.; Černý, R. Fox, ‘Free Objects for Crystallography’: A Modular Approach to Ab Initio Structure Determination from Powder Diffraction. *J. Appl. Crystallogr.* **2002**, *35*, 734–743. [[CrossRef](#)]
47. Rodríguez-Carvajal, J. Recent Advances in Magnetic Structure Determination by Neutron Powder Diffraction. *Phys. B Condens. Matter.* **1993**, *192*, 55–69. [[CrossRef](#)]

Disclaimer/Publisher’s Note: The statements, opinions and data contained in all publications are solely those of the individual author(s) and contributor(s) and not of MDPI and/or the editor(s). MDPI and/or the editor(s) disclaim responsibility for any injury to people or property resulting from any ideas, methods, instructions or products referred to in the content.